Tetrahedron 73 (2017) 1640–1649

Contents lists available at ScienceDirect

Tetrahedron

journal homepage: www.elsevier.com/locate/tet

Unexpected regioselectivity observed in the bromination and epoxidation reactions of *p*-benzoquinone-fused norbornadiene: An experimental and computational study

Selcuk Essiz [a, b], Erdin Dalkilic [a], Ozlem Sari [c, d], Arif Dastan [a, **], Metin Balci [c, *]

[a] Department of Chemistry, Atatürk University, 25240, Erzurum, Turkey
[b] Department of Chemical Engineering, Hakkari University, TR-30000 Hakkari, Turkey
[c] Department of Chemistry, Middle East Technical University, 06800 Ankara, Turkey
[d] Department of Chemistry, Ahi Evran University, 40100 Kırşehir, Turkey

ARTICLE INFO

Article history:
Received 28 November 2016
Received in revised form
26 January 2017
Accepted 6 February 2017
Available online 8 February 2017

Keywords:
Bromination
Epoxidation
Norbornadiene
1,4-Benzoquinone
Electrophilic addition

ABSTRACT

The bromination reaction of *p*-benzoquinone-fused norbornadiene was studied at various temperatures (−78, −50, 0, 25, and 77 °C). At room temperature, the double bonds of the *p*-benzoquinone units were mainly brominated. The double bond of the norbornene unit also underwent a bromination reaction in a yield of only 2%. However, the reaction at −78 °C resulted in the formation of products derived from the attack of bromine on the norbornene double bond with higher charge density. In contrast to the bromination reaction, the epoxidation reaction of the same compound with *m*-chloroperbenzoic acid and dimethyldioxirane exclusively resulted in the formation of products derived from the addition to the double bond of norbornadiene. The regioselectivity observed was investigated and the results were supported by theoretical calculations.

1. Introduction

Bromination of alkenes is an important task in synthetic organic chemistry. Bromine can stereospecifically add to alkenes and form *trans*-adducts which serve as valuable precursors in the synthesis of a variety of organic and organometallic species. The mechanism of electrophilic addition of bromine to alkenes has been intensively studied.[1] The mechanism is based on the formation of a bromonium ion and the formation of a *trans*-addition product by *anti*-attack of bromide or tribromide ion to a cyclic ion.[1,2] On the other hand, the bromination of strained cyclic systems such as norbornadiene (**1**) and benzonorbornadiene (**5**) is more complicated. Addition of bromine to norbornadiene (**1**) at lower temperatures results in the formation of products **2**–**4** derived from Wagner-Meerwein rearrangement and homoallylic conjugation (Scheme 1).[3] The expected *trans*-addition product was not detected.

However, the electrophilic addition of bromine to benzonorbornadiene (**5**) at 10 °C exclusively gave the rearranged product **6** in quantitative yield.[4] In the course of studying the bromination reaction of unsaturated bicyclic systems we noted that the reaction temperature has a dramatic influence on product distribution. When the bromination reaction was carried out at higher temperatures (77–150 °C) the formation of rearranged products was suppressed and 1,2-addition products were formed in high yields.[5] Kobayashi and Miki[6] reacted norbornadiene-fused pyrazine derivatives **7a** with bromine to afford *trans*-adduct **8a** as the major product accompanied by an adduct **9a** derived from Wagner-Meerwein type rearrangement and *cis*-adduct **10a** in a ratio of 20:5:1 (86%), respectively (Scheme 1). On the other hand, treatment of dicyanopyrazine derivative **7b** with bromine resulted exclusively in the formation of a *trans*-adduct, **8b**. Contrary to this finding, a pyrazine-fused norbornadiene with an *N*-oxide electron donating group only gave a rearranged product having the same skeleton as **9**. All this information shows that the charge density on the ring fused to the norbornadiene unit has a dramatic effect on the distribution of the products. As part of our ongoing research on bromination of hydrocarbons we were interested in the bromination reaction of benzoquinone-fused norbornadiene **11** (Fig. 1) to

* Corresponding author.
** Corresponding author.
E-mail addresses: adastan@atauni.edu.tr (A. Dastan), mbalci@metu.edu.tr (M. Balci).

http://dx.doi.org/10.1016/j.tet.2017.02.017
0040-4020/

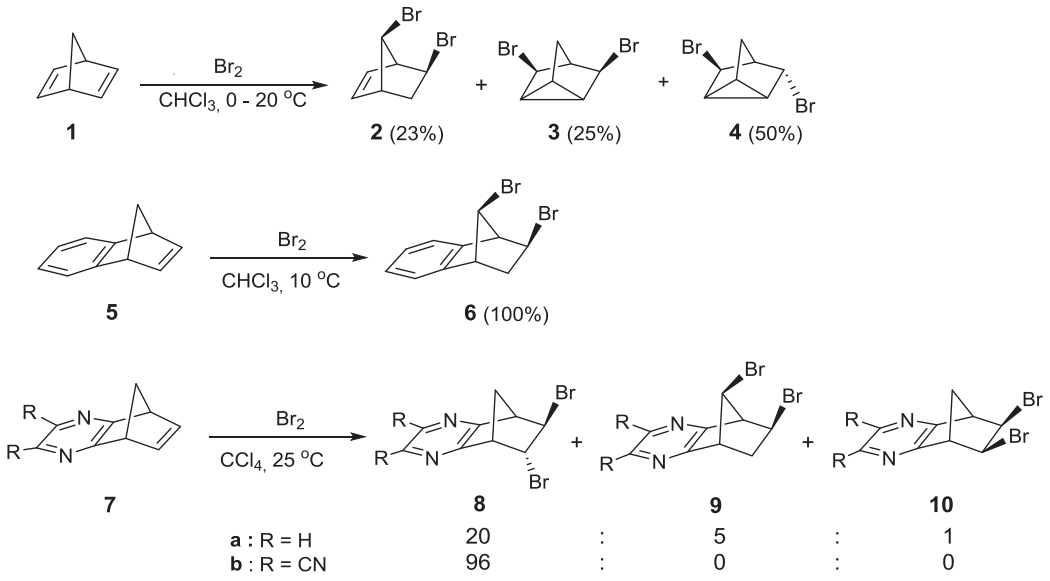

Scheme 1. Bromination of norbornadiene and benzonorbornadiene derivatives **1**, **5**, and **7**.

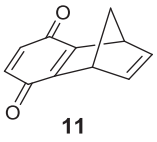

11

Fig. 1. Structure of benzoquinone-fused norbornadiene **11**.

investigate the effect of the *p*-benzoquinone unit on the mode of the reaction. Furthermore, this compound **11** contains three different double bonds that can undergo bromine addition. In this context, we investigated the regioselectivity as well as the stereoselectivity of bromination and epoxidation reactions. Furthermore, the effect of double bond pyramidalization on the outcome of the bromination reaction is discussed.

2. Results and discussion

The starting material, 1,4-methanonaphthalene-5,8(1*H*,4*H*)-dione (**11**), was synthesized as described in the literature.[7] Enedione **12**[8] obtained from the Diels-Alder reaction of 1,4-benzoquinone with cyclopenta-1,3-diene was aromatized over silica gel to afford the corresponding annulated hydroquinone-fused norbornadiene **13**. Subsequent oxidation of **13** with ceric ammonium nitrate (CAN) gave *p*-benzoquinone-annulated norbornadiene **11** in high yield (Scheme 2).

The addition of bromine to **11** was carried out in methylene chloride at various temperatures. The analysis of the ^{1}H NMR spectrum obtained from the reaction at room temperature revealed the presence of two major products **14** and **15**, besides several minor products, **16**–**19** (Scheme 3). The two major products, **14** (47%) and **15** (45%), were separated by crystallization of the reaction mixture from CH_2Cl_2/*n*-hexane. The residue was separated by silica gel column chromatography.

The structures of these compounds were determined on the basis of 1D and 2D (COSY, HSQC, HMBC) spectral data. The dibromides **14** and **19** were characterized easily because of the symmetrical structures, exhibiting six-line ^{13}C NMR spectra. The presence of four double bond proton resonances in the ^{1}H NMR spectra of **14** and **19** clearly indicated the addition of bromine atoms to the central double bond with *cis*-configuration. To distinguish between these isomers (**14** and **19**), we analyzed the ^{1}H NMR chemical shift of the bridge protons. It is well established that the interactions related to the van der Waals effect cause a paramagnetic contribution to the shielding constants. As a consequence of this, the proton resonances are shifted to downfield.[9] The chemical shift difference between the *endo* methylene bridge protons in **14** and **19** ($\Delta\delta = 1.39$ ppm) is very large and considerably meaningful to determine the exact structures. In **14** and **19**, a γ-*gauche* effect was observed depending on the configuration of bromine atoms. The *exo*-orientation of the bromine atoms in **14** causes a remarkable downfield shift of the *endo*-bridge proton (2.59 ppm) because of the steric repulsion caused by bromine atoms (Fig. 2). However, in the case of **19** the *endo*-methylene proton resonance is shifted to upfield (1.10 ppm) due to the presence of this proton in the shielding zone of the double bond as shown in Fig. 2.

The existence of cyclopropane structures in **17** and **18** was determined by measuring the relevant J_{CH} coupling constants in the proton coupled ^{13}C NMR spectra of **17** and **18**. The determined coupling constants J_{CH} (185.2 and 187.5 Hz) in the sp^3-region were decisive for the identification of cyclopropane rings.[10] The configuration of the bromine atoms in **18** was assigned as described above. The downfield chemical shifts of the *endo*-methylene proton (2.50 ppm) as well as the *exo*-methylene proton (2.56 ppm) in **18**

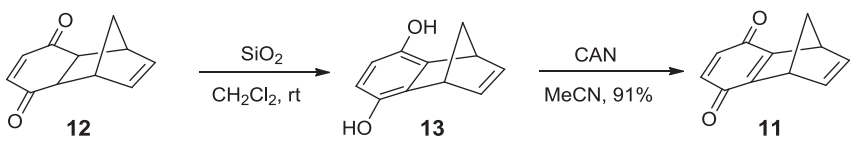

Scheme 2. Synthesis of *p*-benzoquinone-annulated norbornadiene **11**.

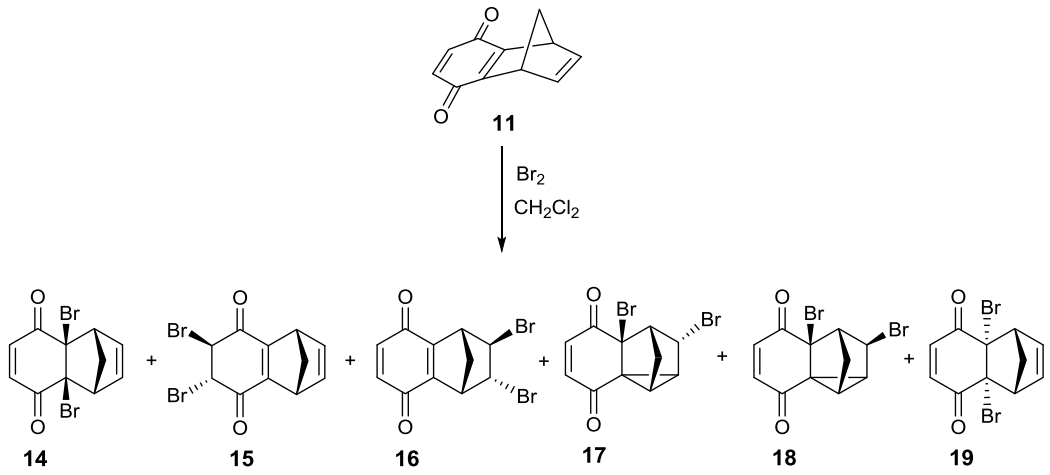

Temperature	Yields in %					
	14	**15**	**16**	**17**	**18**	**19**
77 °C[a]	50	50	-	-	-	-
25 °C[a]	47	45	2	2	1	1
0 °C[b]	44	42	8	2	1	1
-50 °C[b]	-	-	63	17	13	-
-78 °C[b]	-	-	64	15	14	-

[a] Isolated yields, [b] Yields were determined with ^{1}H-NMR spectroscopy

Scheme 3. Bromination of **11** at various temperatures.

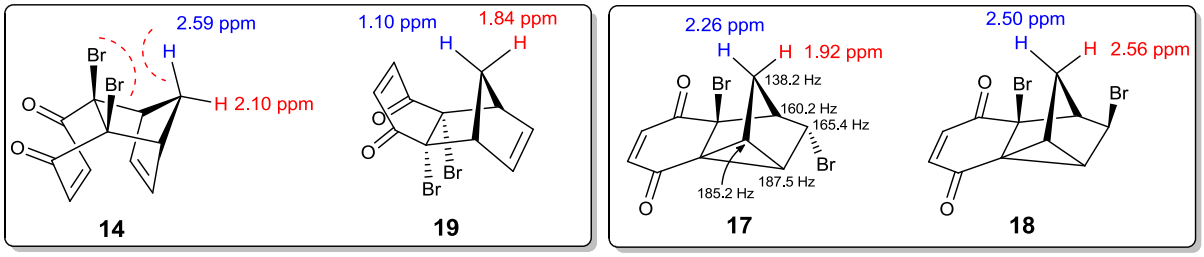

Fig. 2. The ^{1}H NMR data of the methylene protons in **14**, **17**, **18**, and **19** and J_{CH} coupling constants in **17**.

were in agreement with the *exo*-configuration of the bromine atoms. The ^{1}H NMR spectra of the regioisomers **15** and **16** revealed sufficient information for tentative assignments to be made. The 11-line ^{13}C NMR spectra of **15** and **16** in particular confirm the presence of asymmetry in the molecule, in other words, the *trans*-addition of the bromine atom to the corresponding double bonds.

During the column chromatography of the reaction mixture, an additional product **20** was isolated. We noted that this compound was formed on a silica gel column by HBr elimination from the major product **15**. Independently, treatment of pure dibromide **15** with silica gel yielded monobromide **20**[11] in quantitative yield (Scheme 4).

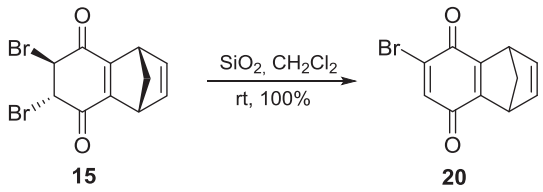

Scheme 4. Formation of **20**.

For the formation of stereoisomers **14** and **19**, we propose the following reaction mechanism. Formation of the products **14** and **19** is unexpected because the electrophilic addition of molecular bromine to a double bond under ionic conditions generally gives *trans*-dibromides. Electrophilic bromine can attack the central double bond from the *endo*- as well as from the *exo*-face of the double bond. It is evident from the configurations of the bromine atoms in **14** that the initial attack occurred from the *exo*-face of the double bond. The formed bromonium ion **21** can rearrange to the non-classical carbocation **22** by an alkyl shift (Scheme 5). The bromide anion present in the reaction media can attack the carbon atoms C-5 (path a) and C-4 (path b) to form **14** and **23**, respectively. The product **14** with *cis*-configuration was formed as one of the major products. However, the product **23** was not formed. We assume that the attack of the bromide ion on the C-4 carbon atom is hindered by the neighboring bromine atom as well as by the *exo*-positioned bridge proton. Compounds **17** and **18**, comprising cyclopropane moieties, may also be formed through the same intermediate **22** by attacking of the bromide anion on the C-2 carbon atom from the *exo*- and *endo*-faces (path c) where a double bond shift is involved. The formation of **19** can be explained by the formation of the *endo*-bromonium ion **24** in the same way (Scheme 5).

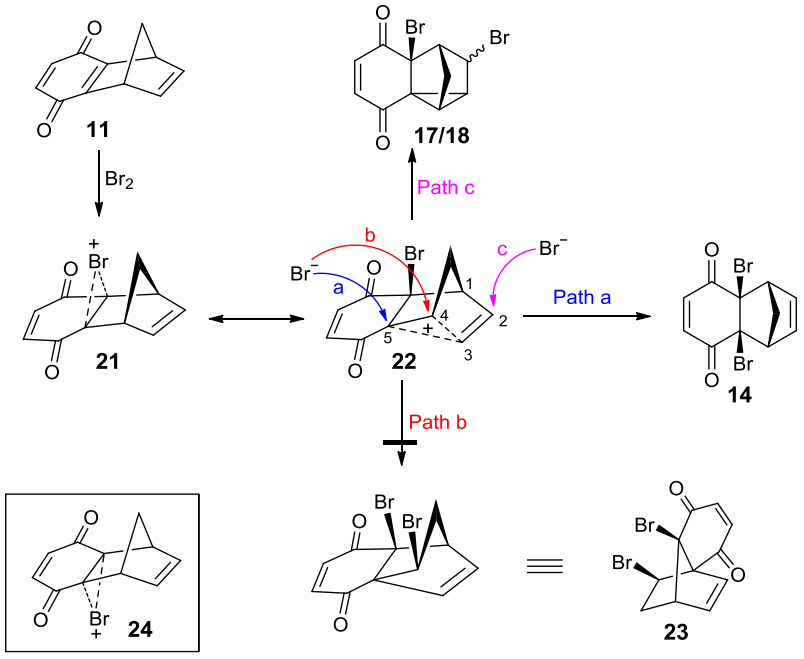

Scheme 5. Mechanisms for formation of **14**, **17**, and **18**.

The configuration of the bromine atoms in **14** shows that the *exo*-attack of bromine on the central double bond is favored. This is due to the pyramidalization of the double bonds in **11**. The double bonds in norbornadiene are pyramidalized in the *endo*-direction.[12] Norbornadiene and related compounds exclusively undergo an *exo*-attack upon treatment with bromine. We calculated the pyramidalization angle of the double bonds in **1** and **11**. We noted that there is no dramatic change in the degree of pyramidalization when going from **1** to **11** (Fig. 3). The double bonds in **11** are *endo*-pyramidalized so that the attack of bromine mainly occurs from the *exo*-face.

To determine the regioselectivity of bromine addition to **11** having three different double bonds, the compound was submitted to a bromination reaction at lower temperatures. Unexpectedly, the reaction at −78 °C gave three products **16**, **17**, and **18** with yields of 64%, 15%, and 14%, respectively (Scheme 3). The major product **16** was formed by *trans*-addition of bromine to the norbornene double bond. The formation of a rearranged product with a structure similar to **9a** was not observed. We assume that the carbonyl groups retarded the formation of a non-classical carbocation. The bromination reaction at −50 °C gave similar results (Scheme 3). However, when the reaction was carried out at 0 °C, the product distribution was completely changed. We obtained products with similar distribution as observed during the reaction at room temperature.

To check the regio- and stereoselectivity of bromine addition to **11**, the bromination reaction was carried out at 77 °C. The high temperature bromination gave two non-rearranged products **14** and **15** in a ratio of 1:1 in quantitative yield (Scheme 3). The mechanism of bromine addition at high temperatures is different than the mechanism at low temperatures. We demonstrated that at high temperatures bromine radicals are involved.[5] Generally, the radicals have a low tendency for rearrangements.

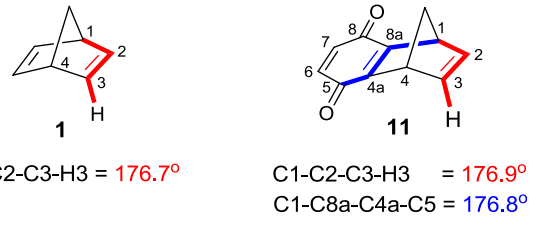

Fig. 3. Pyramidalization angles of optimized molecules at the M06-2X/6-31 + G(d,p) level.

After completion of bromine addition to **11** we focused on the epoxidation reaction of **11** to investigate again regio- and stereoselectivity. The reaction of **11** with *m*-chloroperbenzoic acid (*m*-CPBA) was performed in methylene chloride at room temperature. The ^{1}H NMR spectral studies of the crude product showed the formation of two isomeric epoxides **25** and **26** in almost quantitative yield in a ratio of 4.6:1, respectively (Scheme 6). Similarly, epoxidation of **11** with dimethyldioxirane (DMDO) also resulted in the formation of the same isomeric mixture **25** and **26**, in a ratio of 3:1. Contrary to the bromination reaction of **11**, no trace of epoxidation products derived from oxidation of the quinoid ring was observed.

2.1. Computational methods

To support the unusual behavior of **11** against bromination and epoxidation reactions we performed a series of density functional theory calculations. All calculations were performed using the Gaussian09[13] program. The molecular geometries of all structures for the formation of non-classical carbocations were fully optimized with M06-2X[14] hybrid functional combined with the 6-31 + G(d,p) basis set using the conductor-like polarizable continuum solvation model (CPCM)[15] in DCM.

The epoxidation reaction of triene **11** with *m*-chloroperbenzoic acid (*m*-CPBA) was also investigated with the exchange-correlation functional B3LYP[16] at 6-31 + G(d,p) theory level in the gas phase. In order to include the solvent effect, single-point calculations were carried out at the same level as the geometry optimizations using the CPCM solvation model with DCM since it was used in the experimental study. All stationary points along the reaction paths were verified by harmonic vibrational frequencies calculated using analytical second derivatives at 25 °C and 1 atm.

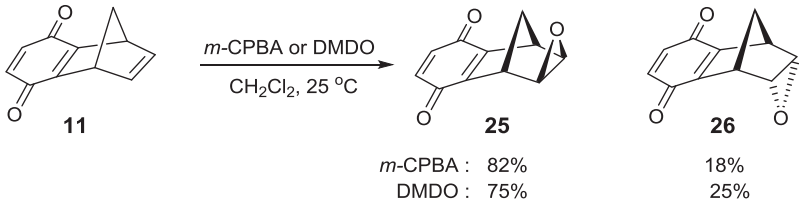

Scheme 6. Epoxidation of **11** with *m*-CPBA and DMDO at room temperature.

Table 1
Calculated relative enthalpy energies of six possible products using M06-2X/6-31 + G(d,p) level in kcal/mol.

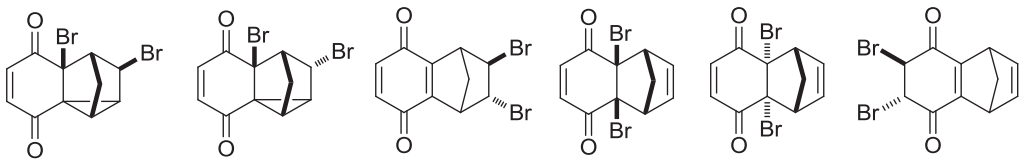

Table 2
Relative enthalpies of the bromine-cation complexes (in kcal/mol) for **21**, **24**, and **27**–**30** using M06-2X/6-31 + G(d,p) level.

Bromine-cation complexes	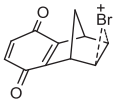 27	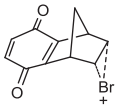 28	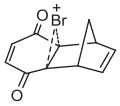 21	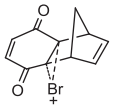 24	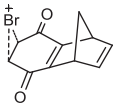 29	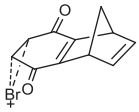 30
Energy differences	-3.5	-1.0	0.0	6.7	18.3	18.9

Intrinsic reaction coordinate (IRC)[17] analysis was performed to ensure that the transition states led to the corresponding minima. Natural bond orbital (NBO)[18] analyses were applied to obtain the atomic charges.

The *p*-quinone-fused norbornadiene **11** has three different double bonds that can be attacked to form a bromonium ion, from the *endo*- as well as the *exo*-faces. First we determined the relative energies of the adducts formed during the reaction of **11** with bromine at room temperature to find whether the thermodynamically most stable compounds were formed as the major product or not (Table 1).

We found that the cyclopropane derivatives **18** and **17** were the thermodynamically most stable compounds followed by **16**. The products **14**, **15**, and **19** derived from the addition of bromine to the *p*-quinone unit are the less stable compounds. To explain the formation of less stable compounds during the bromination reaction

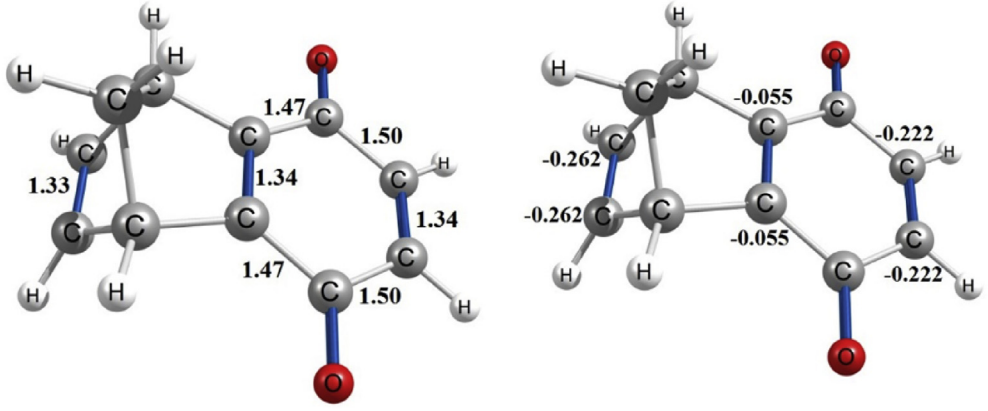

Fig. 4. Geometry optimized structure of **11** and atomic charge distribution (NBO analysis) carried out using the M06-2X method and a basis set 6-31 + G(d,p). Distances are given in Å.

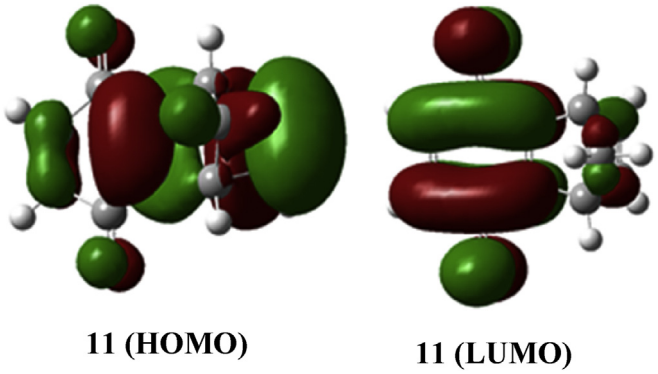

Fig. 5. The calculated highest occupied (HOMO) and lowest unoccupied (LUMO) MOs of **11**.

at room temperature we first determined the relative energies of bromonium ions derived from different attacks (Table 2).

It was found that bromonium ion **21** derived from the *exo*-attack of bromine on the central double bond and **27** and **28** derived from the *exo*- and *endo*-attack on the norbornene double bond are the most stable ones. However, only the formation of **21** was in agreement with the products formed by the bromination reaction of **11** at room temperature. Unfortunately, the product **16** derived from the most stable intermediates **27** and **28**, was isolated in 2% yields. To address the question of why the major products were not formed from the intermediates **27** and **28**, we calculated the charge distribution in **11**. Geometry optimization and frequency calculation of **11** were performed with the M06-2X/6-31 + G(d,p) method. We found that the greater negative charges are located on the C2–C3 and C6–C7 double bond carbon atoms (Fig. 4). Therefore, one would expect that an electrophile, the bromonium ion, would attack the more negatively charged carbon atoms in **11**. The formation of the product **15** is in agreement with the charge distribution. However, an addition product **16** derived from the attack on the norbornene double bond was formed in a yield of only 2%.

Furthermore, we calculated the highest occupied (HOMO) and lowest unoccupied (LUMO) molecular orbitals of **11** shown in Fig. 5. In the case of HOMO, the charge is mainly accumulated on the norbornene double bond. In contrast, the LUMO is located over the benzoquinone ring.

After calculation of the relative energies of the bromonium ion complexes **21** and **27**, we calculated the transition structures for formations of their non-classical carbocations **22** and **31** starting from the *exo*-bromonium ions (Fig. 6). The formation of non-classical carbocations via sigma bond participation was investigated using M06-2X/6-31 + G(d,p) level in DCM. For the formation of **22**, an activation energy of 0.44 kcal/mol (with respect to the energy of **21**) is required (Fig. 7). On the other hand, 2.92 kcal/mol is required for the formation of **31** with respect to the energy of **27** (Fig. 7). Therefore, we assume that the lower activation barrier for the formation of **22** is the driving force of this reaction and is also responsible for the regioselectivity. At low temperature reactions bromine exclusively attacks the norbornene double bond with the higher charge density.

Epoxidation reactions of **11** with *m*-CPBA and DMDO were also theoretically investigated. In contrast to the bromination reaction, epoxidation of **11** took place exclusively on the norbornadiene double bond C2–C3, forming the *exo*- and *endo*-products **25** and **26**; **25** was the major product. In both cases, *exo*-products were the major products (Scheme 6). Interestingly, epoxidation took place only on the norbornadiene double bond. There are three double bonds in **11**, which can be attacked from both sides of the double bonds to give six possible epoxides; **25**, **26**, and **32**–**35**. First, we calculated the relative enthalpies of the six possible isomers at B3LYP/6-31 + G(d,p) level and found that the isomers **25** and **26** were the most thermodynamically stable (Table 3). The formation of **25** as the major product can be explained by the *endo*-pyramidalization of the double bond so that attack from the *exo*-face is preferred. Furthermore, we investigated the activation barriers for the formation of all six possible isomers **25**, **26**, and **32**–**35** in the gas phase and dichloromethane. The values are tabulated in Table 3.

The calculated energy barriers were generally about 1 kcal/mol lower in methylene chloride compared to the gas phase (Table 3). The Gibbs free energy barriers for the formation of **32**–**35** were about 6–10 kcal/mol higher than those for the formation for **25** and **26**. Therefore, epoxidation of the norbornadiene double bond was both thermodynamically and kinetically more favorable (Fig. 8). The optimized structures of TS3 and TS4 are shown in Fig. 8 (for all stationary points, see the Supporting Information). These computational results are in quite good agreement with the experimental findings.

3. Conclusions

The electrophilic addition of bromine to **11** at room temperature led to the formation of two major products **14** and **15**. The *cis*-configuration of the bromides in **14** was explained by the formation of a non-classical carbocation **22** by an alkyl shift. The *exo*-attack was attributed to the double bond pyramidalization. Furthermore, we determined that the lower activation barrier for the formation of **22** is the driving force of this reaction and is also responsible for the regioselectivity although the charge density at the central double bond was lower compared to that of the other double bonds. Reaction at lower temperatures (−50 and −78 °C) gave **16** as the major product arising from the attack of bromine on the norbornene double bond with higher charge density. On the other hand, epoxidation of **11** took place exclusively at the norbornadiene double bond C2–C3, forming the *exo*- and *endo*-products **25** and **26**, where **25** was the major product. The calculated activation barriers showed that the barrier for the formation of **25** and **26** was about 6–10 kcal/mol lower than that for the formation of products **32**–**35**.

4. Experimental section

4.1. General methods

Reactions were monitored using Thin Layer Chromatography (TLC) using aluminium-backed Silica-Gel 60 F254 plates. Column

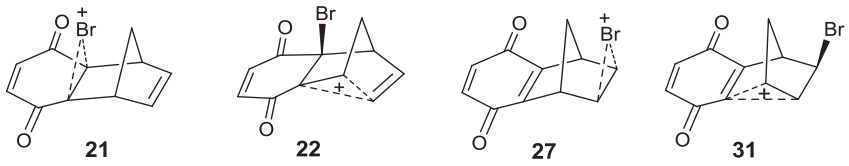

Fig. 6. The structures of intermediates **21**, **22**, **27**, and **31**.

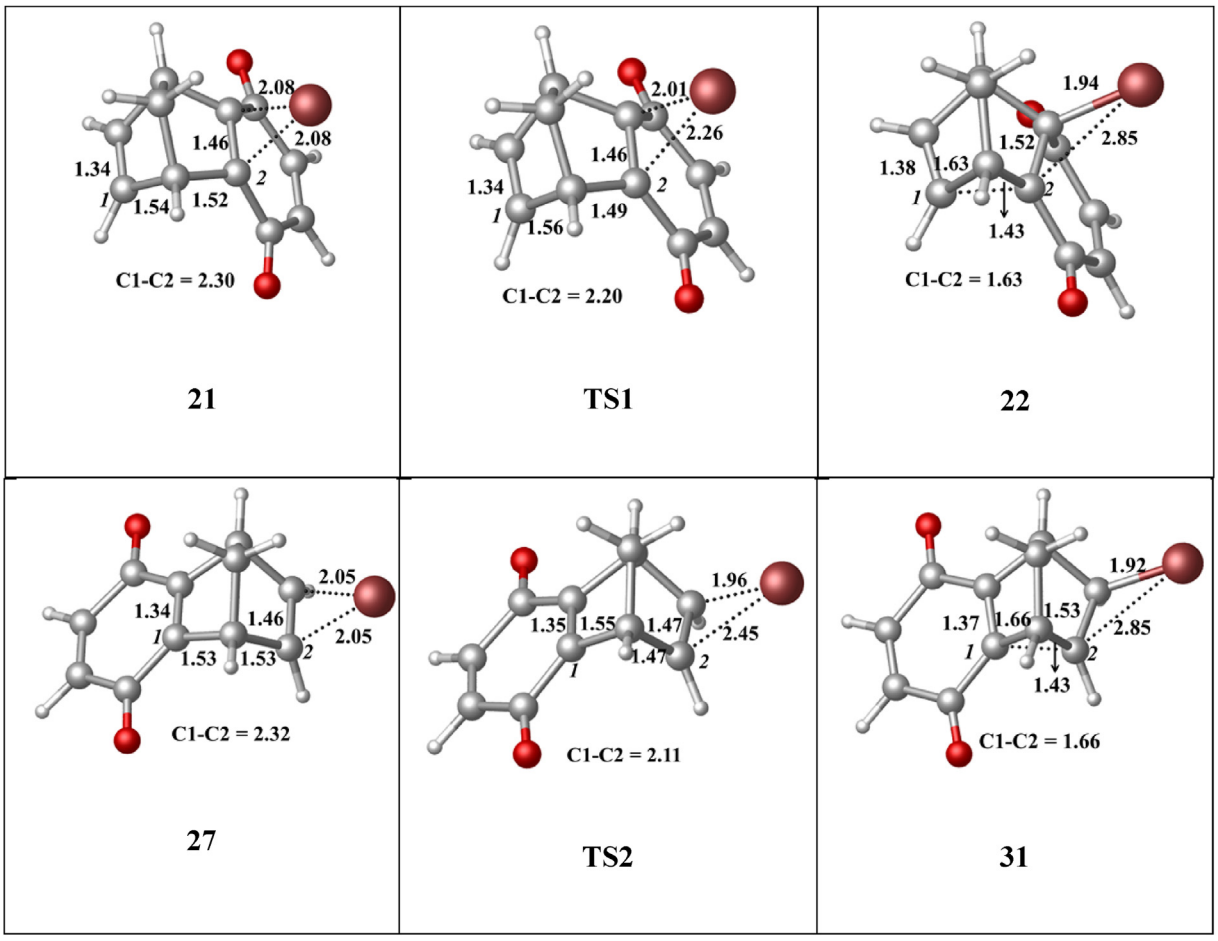

Fig. 7. Optimized geometries of bromonium cation complexes (**21** and **27**), transition states, and non-classical carbocations at the M06-2X/6-31 + G(d,p) level in DCM. Some critical distances (Å) are given.

chromatography was performed using Silica-Gel 60 (Merck). All chromatography was carried out using a combination of *n*-hexane and ethyl acetate as an eluent. Preparative TLC was performed using Silica-Gel 60 HF254 + 366. Infrared spectra were recorded on a Perkin Elmer FT-IR spectrometer with KBr pellets. NMR spectra were recorded using a Bruker and Varian 400 MHz NMR instrument (^{1}H NMR at 400 MHz, ^{13}C NMR at 100 MHz) in $CDCl_3$. All chemical shifts are reported in ppm and *J* values are quoted in Hz. Elemental analyses were recorded on LECO 932 CHNS elemental analyzer. Mass spectra were performed with ThermoFinnigan instrument (EI, 70 eV).

4.2. Synthesis of 1,4-dihydro-1,4-methanonaphthalene-5,8-dione (11)

A solution of freshly distilled cyclopentadiene (6.60 g, 0.10 mol) in dichloromethane (10 mL) was added to a solution of 1,4-benzoquinone (10.80 g, 0.10 mol) in dichloromethane (30 mL) at 0 °C dropwise. Then, the solution was stirred at room temperature for 2 h to give product **12** (17.0 g, 97%). The addition product **12** (10.0 g 57.4 mmol) was dissolved in dichloromethane (50 mL) and silica gel (60-mesh, 50.0 g) was added. The resulting mixture was stirred at room temperature for 0.5 h to promote adsorption of **12** onto the silica gel surface. The resulting suspension was placed onto a silica gel column (100 g, dimensions 80 cm × 3 cm) and then was allowed to stand on the column overnight. The formed hydroquinone derivative **13** was obtained in quantitative yield (10.0 g, 100%) by elution with ethyl acetate/*n*-hexane (1:3) solution. A solution of ceric ammonium nitrate ($Ce(NH_4)_2(NO_3)_6$, 78.70 g, 143.5 mmol) in water (100 mL) was added to a solution of **13** (10.0 g, 57.4 mmol) in CH_3CN (100 mL) at 0 °C and the resulting mixture was stirred at room temperature for 1 h. After adding water (100 mL) the reaction mixture was extracted with ether (3 × 100 mL). The combined organic layers were washed with brine (50 mL), dried over Na_2SO_4, and filtered. The solvent was evaporated under reduced pressure and the residue was purified via column chromatography on silica gel (100 g) by eluting with EtOAc/*n*-hexane (3:17). The product **11** was obtained as a yellow solid (9.0 g, 91%); m.p. 62–64 °C (Lit. m.p. 65–67 °C[7]).

4.3. Bromination of 1,4-dihydro-1,4-methanonaphthalene-5,8-dione (11) at room temperature

To a magnetically stirred solution of **11** (1.72 g, 10.0 mmol) in 30 mL of dry methylene chloride was added a solution of bromine (1.68 g, 10.5 mmol) in methylene chloride (5 mL) at room temperature over a period of 5 min. The resulting reaction mixture was stirred for 10 min. The solvent was evaporated under reduced pressure and the residue was recrystallized from methylene chloride/*n*-hexane (2:1). Major products **14** and **15** were separated. The remaining part was submitted to column chromatography (silica gel, 100 g) eluting with EtOAc/*n*-hexane (1:9). The products were separated in the following order:

Table 3
Relative energies of the possible epoxides **25**, **26**, and **32**–**35** derived from the reaction of *m*-CPBA (in kcal/mol) with **11** at B3LYP/6-31 + G(d,p) level.

Epoxides	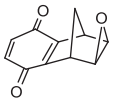	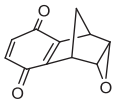	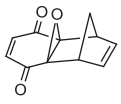	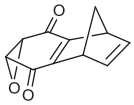	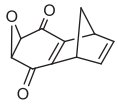	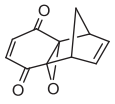
Relative Energies	−10.2[25]	−6.8 [26]	−2.6 [32]	0.0 [33]	−0.4[34]	+1.4[35]
Activation energies in Gas Phase	16.5	18.8	22.9	23.1	23.5	26.7
Activation energies in CH_2Cl_2	14.0	15.9	22.7	22.1	22.5	26.5

4.3.1. rel-(1R,4S)-6-Bromo-1,4-methanonaphthalene-5,8(1H,4H)-dione (20)[11]

(0.525 g, 21%); m.p. 95–96 °C Lit. m.p. 101–103 °C. ^{1}H NMR (400 MHz, $CDCl_3$): δ = 7.09 (s, 1H), 6.90–6.83 (m, 2H), 4.18–4.15 (m, 1H), 4.12–4.09 (m, 1H), 2.35 (dt, A-part of AB system, J = 7.2 and 1.3 Hz, 1H), 2.30 (bd, B-part of AB system, J = 7.2 Hz, 1H). ^{13}C NMR (100 MHz, $CDCl_3$): δ = 181.3, 175.8, 161.7, 160.3, 142.5, 142.4, 136.9, 136.8, 74.0, 49.3, 48.6. IR (KBr, cm^{-1}): $\tilde{\nu}_{max}$ = 3048, 3003, 2975, 2943, 2873, 1700, 1569, 1453, 1360, 1304, 1256, 1218, 1074, 1005, 883. MS (EI, 70 eV): $(MH)^+$ = 252.9/250.9 (35), 171.9 (100), 143.9 (25), 114.7 (20).

*4.3.2. rel-(1R,4S,4aR,8aS)-4a,8a-dibromo-1,4,4a,8a-tetrahydro-1,4-methanonaphthalene-5,8-dione **(14)***

(0.30 g + 1.25 g from crystallization, 47%); m.p. 186–187 °C. ^{1}H NMR (400 MHz, $CDCl_3$): δ = 6.83 (s, 2H), 6.15–6.14 (m, 2H), 3.73–3.71 (m, 2H), 2.59 (bd, A-part of AB system, J = 9.9 Hz, 1H), 2.10 (dt, B-part of AB system, J = 9.9 Hz and J = 1.7 Hz, 1H). ^{13}C NMR (100 MHz, $CDCl_3$): δ = 188.6, 140.6, 137.7, 70.2, 55.2, 45.3. IR (KBr, cm^{-1}): $\tilde{\nu}_{max}$ = 3064, 2992, 2952, 1682, 1365, 1266, 1242, 1099, 987, 905, 857. MS (EI, 70 eV): $(MH)^+$ = 334.9/332.9/331 (50%), 304.8 (75), 252.9/250.9 (60), 224.9/222.9 (60), 143.7 (100), 114.8 (55). Anal. Calcd. for $C_{11}H_8Br_2O_2$: C, 39.80; H, 2.43%. Found: C, 39.67; H, 2.41.

*4.3.3. rel-(1R,4S,4aS,8aR)-4a,8a-dibromo-1,4,4a,8a-tetrahydro-1,4-methanonaphthalene-5,8-dione **(19)***

The dibromide **19** was isolated as a mixture with **14** (33.0 mg, 1%) in a ratio of (2:5). ^{1}H NMR (400 MHz, $CDCl_3$): δ = 6.99 (s, 2H), 6.47–6.46 (m, 2H), 3.93–3.91 (m, 2H), 1.84 (dt, A-part of AB system, J = 11.0 and 1.8 Hz, 1H), 1.16 (bd, B-part of AB system, J = 11.0 Hz, 1H). ^{13}C NMR (100 MHz, $CDCl_3$): δ = 187.4, 140.8, 138.0, 70.3, 51.0, 44.7. IR (KBr, cm^{-1}): $\tilde{\nu}_{max}$ = 3064, 3048, 2986, 2953, 1689, 1603, 1449, 1365, 1265, 1098, 987. MS (EI, 70 eV): $(MH)^+$ = 334.2/332.6/331 (50), 304.9 (75), 253/250.9 (50), 224.9/222.9 (60), 143.8 (100), 115.8/114.7 (70). Anal. Calcd. for $C_{11}H_8Br_2O_2$: C, 39.80; H, 2.43%. Found: C, 39.76; H, 2.38.

*4.3.4. rel-(1aS,2S,3S,3aS,7aR)-2,3a-dibromo-1a,2,3,3a-tetrahydro-1H-1,3-methanocyclo-propa-[c]indene-4,7-dione **(18)***

(34.0 mg, 1%), colorless wax. ^{1}H NMR (400 MHz, $CDCl_3$): δ = 6.82 (d, A-part of AB system, J = 10.5 Hz, 1H), 6.73 (d, B-part of AB system, J = 10.5 Hz, 1H), 4.14 (bs, 1H), 2.97–2.95 (m, 1H), 2.89 (bd, J = 5.1 Hz, 1H), 2.56 (bd, A-part of AB system, J = 12.0 Hz, 1H), 2.50 (bd, B-part of AB system, J = 12.0 Hz, 1H), 2.30 (dt, J = 5.1 and 1.0 Hz, 1H). ^{13}C NMR (100 MHz, $CDCl_3$): δ = 190.1, 188.7, 141.1, 139.4, 66.1, 46.3, 45.9, 41.2, 37.7, 31.6, 23.0. IR (KBr, cm^{-1}): $\tilde{\nu}_{max}$ = 3081, 2958, 2964, 1689, 1586, 1455, 1393, 1295, 1259, 1126, 1039, 982, 851. MS (EI, 70 eV): m/z 333/330.9 (35), 251/252.3 (100), 222.9 (25), 170.9 (70), 146.8 (25). Anal. Calcd. for $C_{11}H_8Br_2O_2$: C, 39.80; H, 2.43%. Found: C, 39.86; H, 2.65.

*4.3.5. rel-(1aS,2R,3S,3aS,7aR)-2,3a-dibromo-1a,2,3,3a-tetrahydro-1H-1,3-methanocyclo-propa-[c]indene-4,7-dione **(17)***

(60.0 mg 2%). Colorless wax. ^{1}H NMR (400 MHz, $CDCl_3$): δ = 6.77 (d, A-part of AB system, J = 10.6 Hz, 1H), 6.69 (d, B-part of AB system, J = 10.6 Hz, 1H), 4.86 (bs, 1H), 3.04 (d, J = 5.2 Hz, 1H), 2.92–2.91 (m, 1H), 2.26 (bd, A-part of AB system, J = 12.6 Hz, 1H),

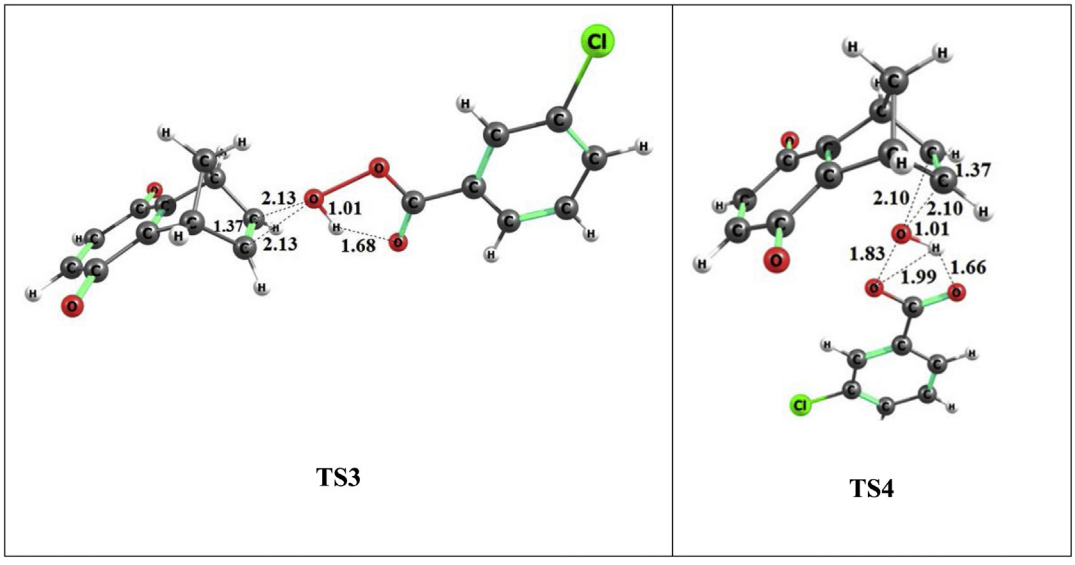

Fig. 8. Optimized geometries of transition states for the formation of **25** and **26** at the B3LYP/6-31 + G(d,p) level. Some critical distances (Å) are given.

2.15 (dd, $J = 5.2$ Hz and 1.1 Hz, 1H), 1.92 (bd, B-part of AB system, $J = 12.6$ Hz, $1H_e$). ^{13}C NMR (100 MHz, $CDCl_3$): $\delta = 190.1, 187.9, 140.7, 138.7, 68.2, 52.1, 46.1, 41.3, 32.6, 29.4, 28.8$. IR (KBr, cm^{-1}): $\tilde{\nu}_{max} = 3048, 2958, 2924, 2846, 1701, 1587, 1459, 1400, 1256, 1123, 1088, 1016, 910, 851$. MS (EI, 70 eV): $(MH)^+ = 333/334.3$ (20), 253.1/252.3/254.1 (50), 171/173 (60), 146.8 (100), 114.9 (20). Anal. Calcd. for $C_{11}H_8Br_2O_2$: C, 39.80; H, 2.43%. Found: C, 39.70; H, 2.66.

4.3.6. rel-(1R,2R,3R,4S)-2,3-dibromo-1,2,3,4-tetrahydro-1,4-methanonaphthalene-5,8-dione **(16)**

(70.0 mg, 2%). Colorless wax. ^1H NMR (400 MHz, $CDCl_3$): $\delta = 6.71$ (bs, 2H), 4.58 (dd, $J = 3.8$ and 2.5 Hz, 1H), 3.87–3.83 (m, 2H), 3.72–3.69 (m, 1H), 2.38 (dt, A-part of AB system, $J = 10.3$ and 1.2 Hz, 1H), 2.16 (ddt, B-part of AB system $J = 10.3$, 2.5, and 1.7 Hz, 1H). ^{13}C NMR (100 MHz, $CDCl_3$): $\delta = 183.3, 183.0, 151.4, 148.8, 136.4, 136.3, 53.8, 52.3, 50.2, 49.5, 46.2$. IR (KBr, cm^{-1}): $\tilde{\nu}_{max} = 3053, 2986, 2956, 2880, 1657, 1584, 1495, 1458, 1399, 1322, 1175, 1084, 1015, 960$. MS (EI, 70 eV) $(MH)^+ = 334.9/332.9/330.8$ (30), 252.8/253.9 (40), 224.9 (10), 170.9 (50), 146.8/145.8 (100), 114.8 (10). Anal. Calcd. for $C_{11}H_8Br_2O_2$: C, 39.88; H, 2.36; Found: C, 39.80; H, 2.43%.

4.3.7. rel-(1R,4S,6S,7S)-6,7-dibromo-6,7-dihydro-1,4-methanonaphthalene-5,8(1H,4H)-dione **(15)**

(0.80 g + 0.70 g from crystallization) 45%; m.p.139–140 °C. ^1H NMR (400 MHz, $CDCl_3$) $\delta = 6.92$ (dd, A-part of AB system, $J = 4.0$ Hz and 3.1 Hz, 1H), 6.89 (dd, B-part of AB system, $J = 4.0$ Hz and 3.1 Hz, 1H), 4.79 (d, A-part of AB system, $J = 2.8$ Hz, 1H), 4.77 (d, B- part of AB system, $J = 2.7$ Hz, 1H), 4.14 (bs, 1H), 4.07 (bs, 1H), 2.38–2.36 (bs, 2H). ^{13}C NMR: $\delta =$ (100 MHz, $CDCl_3$) $\delta = 184.4, 183.8, 161.23, 161.16, 142.2141.7, 73.3, 49.2, 49.1, 47.4, 46.6$. IR (KBr, cm^{-1}): $\tilde{\nu}_{max} = 2980, 2936, 2868, 1675, 1583, 1561, 1362, 1281, 1222, 1197, 1150$. MS (EI, 70 eV): m/z 252.9/251.0 (M^+-Br, 50), 171.8 (100), 143.8/142.7 (35), 114.7 (20). Anal. Calcd. for $C_{11}H_8Br_2O_2$: C, 39.80; H, 2.43%. Found: C, 39.94; H, 2.49.

4.4. Bromination of 1,4-dihydro-l,4-methanonaphthalene-5,8-dione (11) at 0, −50 and −78 °C

To a magnetically stirred solution of **11** (0.344 g, 2.0 mmol) in 10 mL of dry methylene chloride at 0, -50 or −78 °C was added a solution of bromine (336.0 mg, 2.1 mmol) in 2 mL of dry methylene chloride over a period of 5 min. The resulting reaction mixture was allowed to warm up to room temperature and the solvent was evaporated. The product ratio was determined by ^1H NMR analysis.

4.5. Bromination of 1,4-dihydro-1,4-methanonaphthalene-5,8-dione (11) at 77 °C

A hot (~60 °C) solution of bromine (0.335 g, 2.10 mmol) in carbon tetrachloride (CAUTION: toxic!) (2 mL) was added to a magnetically stirred solution of **11** (345 mg, 2.0 mmol) in carbon tetrachloride (10 mL) at reflux in a 25 mL flask, over a period of 2 min. The resulting reaction mixture was kept at reflux temperature for 5 min. After evaporation of the solvent the residue was chromatographed on silica gel (30.0 g), eluting with EtOAc/*n*-hexane (1:9) to give **20** (251.0 mg, 50%) as the first fraction. The compound **14** (332 mg, 50%) was isolated as the second fraction.

4.6. Reaction of 1,4-dihydro-l,4-methanonaphthalene-5,8-dione (11) with m-chloroperbenzoic acid (m-CPBA) at 0 °C

To a magnetically stirred solution of **11** (0.345 g, 2.0 mmol) in methylene chloride (10 mL) at was added *m*-CPBA (0.380 g, 2.20 mmol) portionwise at 0 °C. The reaction mixture was stirred for 15 h at room temperature. After adding water (25 mL), the mixture was extracted with methylene chloride (3 × 20 mL). The combined organic layers were washed with saturated brine (2 × 10 mL), water, dried over Na_2SO_4, and filtered. The solvent was removed in *vacuo*. The residue was purified via column chromatography on silica gel (30.0 g) by eluting with EtOAc/*n*-hexane (3:17). The monoepoxides **25** and **26** were separated.

4.6.1. rel-(1aR,2R,7S,7aS)-1a,2,7,7a-tetrahydro-2,7-methanonaphtho[2,3-b]oxirene-3,6-dione **(25)**

The epoxide **25** was isolated as the first fraction. Orange solid (0.310 g, 82%) decom. >120 °C. ^1H NMR (400 MHz, $CDCl_3$): $\delta = 6.65$ (s, 2H), 3.59–3.58 (m, 2H), 3.58–3.57 (m, 2H), 1.97 (bd, A-part of AB system, $J = 9.2$ Hz, 1H), 1.58 (bd, B-part of AB system, $J = 9.2$ Hz, 1H). ^{13}C NMR (100 MHz, $CDCl_3$): $\delta = 183.8, 157.4, 136.0, 57.6, 42.5, 39.9$. IR (KBr, cm^{-1}): $\tilde{\nu}_{max} = 3048, 3008, 2971, 2353, 2336, 1650, 1572, 1499, 1446, 1379, 1315, 1278, 1231, 1194, 1136, 1077, 999$. MS (EI, 70 eV): $(MH)^+ = 188.9$ (5), 170.9/172 (100) 158.9/159.9/160.9 (100), 142.8 (30), 130.8/132.8/133.9 (80), 114.8/117 (75), 102.8/103.7/104.7 (60), 77(10). Anal. Calcd. for $C_{11}H_8O_3$: C, 70.21; H, 4.29%. Found: C,70.53; H, 4.21.

4.6.2. rel-(1aR,2S,7R,7aS)-1a,2,7,7a-tetrahydro-2,7-methanonaphtho[2,3-b]oxirene-3,6-dione **(26)**

The epoxide **26** was isolated as the second fraction. Orange solid (66.0 mg 18%), decom. >160 °C: ^1H NMR (400 MHz, $CDCl_3$): $\delta = 6.65$ (s, 2H), 3.92 (d, $J = 3.0$ Hz, 2H), 3.45–3.43 (m, 2H), 2.33 (dt, A-part of AB system, $J = 8.9$ and 1.6 Hz, 1H), 2.22 (bd, B-part of AB system, $J = 8.9$ Hz, 1H). ^{13}C NMR (100 MHz, $CDCl_3$): $\delta = 184.3, 146.6, 136.2, 60.5, 52.7, 41.8$. IR (KBr, cm^{-1}): $\tilde{\nu}_{max} = 2952, 2913, 2857, 2347, 1656, 1575, 1455, 1357, 1264, 1055$. MS (EI, 70 eV): $(MH)^+ = 188.7$ (20), 170.9/172 (100), 158.9/160.2/161 (80), 142.9 (20), 130.9/133 (30), 114.7/117.1 (25), 102.9 (20), 76.7 (20). Anal. Calcd. for $C_{11}H_8O_3$: C, 70.21; H, 4.29%. Found: C, 70.38; H, 4.42.

4.7. Preparation of dimethyldioxirane (DMDO)[19]

Sodium bicarbonate (29.0 g, 345.0 mmol) was dissolved in 225 mL of acetone-water (4:5/225 mL) at 5 °C. Potassium peroxymonosulfate (60.0 g, 195.0 mmol) was added to the solution in five portions at 3 min intervals. After 5 min the cooling bath was removed and a moderate vacuum (80–100 torr) was applied while vigorously stirring. The DMDO/acetone distillate was collected in the cooled (−78 °C) receiving flask. (The concentration of DMDO can be determined by oxidation of methyl phenyl sulfide to its sulfoxide.)

4.8. Reaction of 1,4-dihydro-l,4-methanonaphthalene-5,8-dione (11) with DMDO

To a magnetically stirred solution of **11** (0.10 g, 0.58 mmol) in 10 mL of methylene chloride was added a solution (excess amount) of DMDO/acetone (25 mL, 0.58 mmol) dropwise at −30 °C. The cooling bath was removed and the reaction mixture was stirred for 30 min at room temperature. The solvent was removed under reduced pressure and the residue was purified via column chromatography on silica gel (20.0 g) eluting with EtOAc/*n*-hexane (3:17). The products **25** and **26** were obtained in quantitative yield in a ratio 3:1, respectively.

Acknowledgments

Financial support from Atatürk University (Grant no. BAP 2010/33), the Turkish Academy of Sciences, and the Middle East Technical University is gratefully acknowledged. We would also like to thank to Prof. Cavit Kazaz for NMR spectra.

Appendix A. Supplementary data

Supplementary data related to this article can be found at http://dx.doi.org/10.1016/j.tet.2017.02.017.

References

1. (a) Saikia I, Borah J, Phukan P. *Chem Rev*. 2016;116:6837–7042;
   (b) Cresswell AJ, Eey T-CS, Denmark SE. *Angew Chem Int Ed*. 2015;54:15642–15682;
   (c) Eissen M, Lenoir D. *Chem Eur J*. 2008;32:9830–9841;
   (d) De La Mare PBD, Bolton R. *Electrophilic Additions to Unsaturated Systems*. second ed. New York: Elsevier; 1982:136–197;
   (e) Brown RS. *Acc Chem Res*. 1997;30:131–137;
   (f) Ruasse M-F. *Adv Phys Org Chem*. 1993;28:207–291;
   (g) Lenoir DC, Chiappe. *Chem Eur J*. 2003;9:1037–1044.
2. Barkhash VA. *Topp Cur Chem*. 1984;115–117:1–265.
3. (a) Tutar A, Taskesenligil Y, Cakmak O, Abbasoglu R, Balci M. *J Org Chem*. 1996;61:8297–8300;
   (b) Winstein S. *J Am Chem Soc*. 1961;83:1616–1617.
4. (a) Geoghegan K, Smullen S, Evans P. *J Org Chem*. 2013;78:10443–10451;
   (b) Dastan A, Demir U, Balci M. *J Org Chem*. 1994;59:6534–6538;
   (c) Wittig G, Knauss E. *Chem Ber*. 1958;91:895–907;
   (d) Cristol SJ, Nachtigall GW. *J Org Chem*. 1967;32, 3727–3237;
   (e) Wilt JW, Gutman G, Ranus WJ, Zigman AR. *J Org Chem*. 1967;32:893–901;
   (f) Wilt JW, Chenier PJ. *J Org Chem*. 1970;35:1562–1570.
5. (a) Taskesenlioglu S, Dastan A, Dalkilic E, Guney M, Abbasoglu R. *New J Chem*. 2010;34:141–150;
   (b) Sengul ME, Gultekin DD, Essiz S, Sahin E, Dastan A. *Tetrahedron*. 2009;65:4859–4865;
   (c) Daştan A. *Tetrahedron*. 2001;57:8725–8732;
   (d) Gultekin DD, Taskesenligil Y, Dastan A, Balci M. *Tetrahedron*. 2008;64:4377–4383;
   (e) Balci M, Guney M, Dastan A, Azizoglu A. *J Org Chem*. 2007;72:4756–4762;
   (f) Dastan A, Balci M. *Tetrahedron*. 2005;61:5481–5488;
   (g) Horasan N, Kara Y, Azizoglu A, Balci M. *Tetrahedron*. 2003;59:3691–3699;
   (h) Dastan A, Balci M, Hokelek T, Ulku D, Buyukgungor O. *Tetrahedron*. 1994;50:10555–10578;
   (i) Cakmak O, Balci M. *J Org Chem*. 1988;54:181–187.
6. Kobayashi T, Miki K. *Bull Chem Soc Jpn*. 1998;71:1443–1449.
7. Marchand AP, Alihodzic S, Shukla R. *Synth Commun*. 1998;28:541–546.
8. Mal D, Ray S. *Eur J Org Chem*. 2008:3014–3020.
9. (a) Balci M. *Basic ^{1}H- and ^{13}C-nmr Spectroscopy*. Elsevier; 2005:71–73;
   (b) Kazaz C, Dastan A, Balci M. *Magn Reson Chem*. 2005;43:75–81;
   (c) Gheorghiu MD, Olteanu E. *J Org Chem*. 1987;52:5158–5162.
10. Balci M. *Basic ^{1}H- and ^{13}C-nmr Spectroscopy*. Page 325. Elsevier; 2005.
11. Morisso FDP, Wagner K, Horner M, Burrow RA, Bortoluzzi AJ, Costa VEU. *Synthesis*. 2000:1247–1252.
12. (a) Saracoglu N, Talaz O, Azizoglu A, Watson WH, Balci M. *J Org Chem*. 2005;70:5403–5408;
   (b) Can H, Zahn D, Balci M, Brinkman J. *Eur J Org Chem*. 2003:1111–1117;
   (c) Borden WT. *Chem Rev*. 1989;89:1095–1109.
13. Frisch MJ, Trucks GW, Schlegel HB, et al. *Gaussian 09, Revision E.01*. Wallingford CT: Gaussian, Inc.; 2009.
14. (a) Zhao Y, Truhlar DG. *Theor Chem Acc*. 2008;120:215–241;
   (b) Zhao Y, Truhlar DG. *Acc Chem Res*. 2008;41:157–167.
15. (a) Klamt A, Schüürmann G. *J Chem Soc Perkin Trans*. 1993;2:799–805;
   (b) Andzelm J, Kölmel C, Klamt A. *J Chem Phys*. 1995;103:9312–9320;
   (c) Barone V, Cossi M. *J Phys Chem A*. 1998;102:1995–2001;
   (d) Cossi M, Rega N, Scalmani G, Barone V. *J Comput Chem*. 2003;24:669–681.
16. (a) Becke AD. *J Chem Phys*. 1993;98:5648–5652;
   (b) Lee C, Yang W, Parr RG. *Phys Rev B*. 1988;37:785–789.
17. (a) Gonzalez C, Schlegel HB. *J Chem Phys*. 1989;90:2154–2161;
   (b) Gonzalez C, Schlegel HB. *J Phys Chem*. 1990;94:5523–5527.
18. Reed AE, Curtiss LA, Weinhold F. *Chem Rev*. 1988;88:899–926.
19. Adam W, Bialas J, Hadjiarapoglou L. *Chem Ber*. 1991;124:2377.